Semiconductor Physics, Quantum Electronics & Optoelectronics. 2004. V. 7, N 1. P. 43-51.

PACS: 72.15.Gd; 72.20.My; 73.61.Ga

Ferromagnetism induced in diluted $A_{1-x}Mn_xB$ semiconductors

V.P. Bryksa[1], G.G. Tarasov[2], W.T. Masselink[2], W. Nolting[2], Yu.I. Mazur[3], G.J. Salamo[3]

[1]*V. Lashkaryov Institute of Semiconductor Physics, NAS of Ukraine, 41, Prospect Nauki, 03028 Kyiv, Ukraine*
[2]*Humboldt Universitat zu Berlin, Institut fur Physik, Newtonstrasse 15, 2489 Berlin, Germany*
[3]*Department of Physics, University of Arkansas, Fayetteville, Arkansas 7270*

Abstract. Theoretical model has been developed for analysis of the peculiarities of new type of magnetism in diluted magnetic $A_{1-x}Mn_xB$ semiconductors. The coherent potential is introduced using the dynamic mean field theory (DMFT) approximation and the Baym- Kadanoff hypothesis valid for the case $x < x_c$ (x_c is the percolation limit).

Keywords: diluted magnetic semiconductors, ferromagnetism, coherent potential, exchange interaction.

Paper received 05.03.04; accepted for publication 30.03.04.

1. Introduction

It is reckoned traditionally that the description of diluted magnetic semiconductors (DMS) is suitable to start with the Vonsovskii Hamiltonian. Such approach has proved to be efficient in the case of magnetic semiconductors [1, 2]. However, in the opposite case of strongly diluted magnetic $A_{1-x}Mn_xB$ semiconductors, where the electron scattering caused by the structural disorder is of great importance, the traditional scheme of investigation [1, 2] has to be altered.

It has been proposed [3] to use the technique of a coherent potential for determination of the averaged electron Green's function with the self-energy part that is a single node like. Then the ensemble over the spin projections can be introduced and the configuration averaging in the sub-space of spin projections for the transference matrix can be performed thus allowing the coherent potential approximation (CPA) to be closed self-consistently in the zeroth-order approximation. The numerical solution of the corresponding equations shows a significant difference in the density-of-states (DOS) for the opposite directions of the electron spin in the conduction band.

The peculiarities of the electron spectrum of the semiconductors with a chaotic distribution over the magnetic sub-system have been studied by R.N. Bhatt et al [4,5] introducing the paramagnetism of the semiconductor rather as an experimental fact. The diluted magnetic semiconductors have been considered also as the strongly correlated systems [6–8] allowing the principal mechanism of the ferromagnetism to be the double exchange through the resonant energy levels and the levels caused by the broken bonds due to the presence of deep Mn states [9].

In this paper, we derive the equations for the electron Green's functions basing on the CPA for the randomly distributed ions of transition metals in DMS. A number of simplifications that are not crucial for the formation of the energy spectrum of DMS are made. It is assumed the "cluster" scheme with the energy in the conduction band that corresponds to the anti-binding energy ε_A whereas the energy in the valence band is the binding energy ε_B. The energy bands in the tight-binding approximation are formed through the integrals of transfer $t_{\alpha,\beta}$ ($\alpha, \beta = A, B$). Since the Mn ion has the stable half-filled d^5 shell that forms the localized spin momentum , an electron can not be immediately localized in the state. Moreover, the Mn presence in the $A_{1-x}Mn_xB$ semiconductor generates the resonant and broken bonds with the energy ε_{Mn} [9]. For the correct description of the electron sub-system of the semiconductor, it is necessary to take into account the field of the nearest surrounding. We assume that the crystal lattice (of the zinc blend structure) is composed of two sub-lattices: one is the sub-lattice of A atoms and the substitutional atoms (Mn atoms), and another is the sub-lattice of B atoms. The conduction band is formed basically from the s states of the $A_{1-x}Mn_x$ sub-lattice, and the valence band is formed from the p states of the sub-lattice B in the $A_{1-x}Mn_xB$ compound. First the averaged Green's function and the DOS function are determined for the $A_{1-x}Mn_x$ sub-lattice, the atoms of which are in the crystal field created by the B atoms. Then the analogous calculations are performed for the B sub-lattice, the atoms of which are in the random field of A and Mn atoms. Determination of the Green's functions for both sub-lattices has to be self-consistent. The general form of the Hamiltonian for the $A_{1-x}Mn_xB$ compound is given in Section 2

using the technique of projective operators. The electron propagator is found in Section 3 using the graph technique in the Hubbard-I approximation. The configuration averaging of the Green's functions is performed and standard CPA equations are written in Section 4. Section 5 presents the results of numerical solution of the CPA equations. The discussion of these results is given in the concluding Section 6.

2. The model Hamiltonian for general problem of DMS

In general case the Hamiltonian of strongly diluted magnetic semiconductor (SDMS) can be written in the cluster approximation as

$$\hat{H} = \sum_i \hat{H}_i + \sum_{<i,j>,\sigma} t_{ij} a^+_{i\sigma} a_{j\sigma} , \tag{1}$$

where the single node part $\hat{H}_i$ of the Hamiltonian has the Kondo-like form [1, 2],

$$\hat{H}_i = \sum_{\sigma=(+,-)} \varepsilon^i a^+_{i\sigma} a_{i\sigma} + \\ + \sum_{\sigma,\sigma'} \alpha_i (\vec{S}_i \vec{\sigma})_{\sigma\sigma'} a^+_{i\sigma} a_{i\sigma'} + \sum_{\sigma} L^{lat}_i a^+_{i\sigma} a_{i\sigma} . \tag{2}$$

Here $a^+_{i\sigma}$ and $a_{i\sigma}$ are the creation and annihilation operators, respectively, for an electron with the spin σ at the i-th node.

For the energy at the i-th node one has:

$$\varepsilon^i = \sum_{k\in\{A,Mn,B\}} \varepsilon_k X^{kk}_i . \tag{3}$$

The crystal field energy is given by

$$L^{lat}_i = \sum_k \sum_l \sum_{i\neq j} X^{kk}_i \lambda^{kl}_{ij} X^{ll}_j \tag{4}$$

with

$$\lambda^{kl}_{ij} = \int \varphi^*_{ki}(\vec{r}) U_l(\vec{r} - \vec{R}_j) \varphi_{ki}(\vec{r}) d\vec{r} .$$

The $U_l(\vec{r} - \vec{R}_i)$ term is the potential energy of the electron at the point $\vec{r}$ near the node defined by the radius-vector $\vec{R}_i$. The cluster wave functions $\varphi_{ki}(\vec{r})$ are constructed from the atom functions localized at the i-th node the sort of κ and possess the tetrahedral symmetry T_d [9].

The transfer matrix is written as

$$t_{ij} = \sum_{kk'} t_{kk'} X^{kk}_i X^{k'k'}_j . \tag{5}$$

The exchange interaction constant is defined by

$$\alpha_i = \sum_k \sum_{k'\neq k} \sum_j X^{kk}_i \alpha^{kk'}_{ij} X^{k'k'}_j , \tag{6}$$

with

$$\alpha^{kk'}_{ij} = \int \varphi^*_{ki}(\vec{r}) \varphi^*_{k'j}(\vec{r}') \frac{1}{|\vec{r} - \vec{r}'|} \varphi_{ki}(\vec{r}') \varphi_{k'j}(\vec{r}') d\vec{r} d\vec{r}' . \tag{7}$$

The projective operator takes the meaning 1 if the i-th node is occupied by the k atom ($k\in$ (A, Mn, B)) and the meaning 0 in other case.

3. Green's functions for the $A_{1-x}Mn_x$ sub-lattice

The Hamiltonian (1) written in terms of projective operators X^{kk}_i can be rewritten in the interaction representation considering the $A_{1-x}Mn_x$ sub-lattice in the crystal field of the B sub-lattice. In what follows we allow the k index of projective operators to be $k \in \{A, Mn\}$ and assume that the matrix of electronic transfer determines the conduction band half-width in the $A_{1-x}Mn_xB$ semiconductor.

Thus the Hamiltonian (1) reduces to the form of

$$\hat{H} = \hat{H}_o + \hat{H}_{\rm int} , \tag{8}$$

where the $\hat{H}_0$ term represents a single node part and

$$\hat{H}_{\rm int}(\tau) = \sum_{i,\sigma} L^{lat}_i \tilde{a}^+_{i\sigma}(\tau) \tilde{a}_{i\sigma}(\tau) + \\ + \sum_{<ij>,\sigma} t_{ij} \tilde{a}^+_{i\sigma}(\tau) \tilde{a}_{j\sigma}(\tau). \tag{9}$$

The operators $\tilde{a}_{i\sigma}(\tau)$ are given by $\tilde{a}_{i\sigma}(\tau) = e^{\tau\hat{H}_0} a_{i\sigma} e^{-\tau\hat{H}_0}$.

In order to find the Green's functions the averages like the

$$< ... >_a = Z^{-1}(X) Sp_a(...e^{-\beta\hat{H}}) \tag{10}$$

have to be calculated. The technique similar to that developed in Ref. [10–13] is used for calculation of the Green's function

$$G^{\sigma}_X(i1\tau1; i2\tau2) = - < T_\tau \tilde{a}_{i1\sigma}(\tau1) \tilde{a}^+_{i2\sigma}(\tau2) >_a = \\ = - < \sigma(\beta, X) >^{-1}_{0a} < T_\tau \tilde{a}_{i1\sigma}(\tau1) \tilde{a}^+_{i2\sigma}(\tau2) \sigma(\beta, X) >_{0a}, \tag{11}$$

with

$$\sigma(\beta, X) = T_\tau \exp\left\{ - \int_0^\beta \hat{H}_{\rm int}(\tau) d\tau \right\} . \tag{12}$$

If one expands the operator $\sigma(\beta, X)$ in the power series with respect to $\hat{H}_{\rm int}$, using the Hubbard-I approximation [15, 16, 22], the graphical equation for the Green's function can be written as follows

$G^{\uparrow}_X(i1\tau1; i2\tau2) =$ 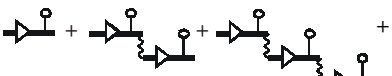 (13)

$G^{\downarrow}_X(i1\tau1; i2\tau2) =$ 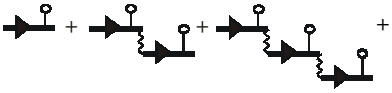 (14)

with

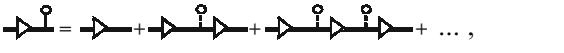 (15)

and

 (16)

Here the graphical notations are used as follows:

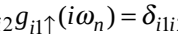 $\equiv \delta_{i1i2} g_{i1\uparrow}(i\omega_n) = \delta_{i1i2} \sum_k g^k_{i1\uparrow}(i\omega_n) X^{kk}_{i1}$ is the electron propagator with the spin-up expressed through the

self-energy part $\Sigma^{\uparrow}{}_{i(k)}(i\omega_n)$ of the electron scattering by the magnetic sub-system.

$\equiv \delta_{i1i2} g_{i1\downarrow}(i\omega_n) = \delta_{i1i2} \sum_k g^k_{i1\downarrow}(i\omega_n) X^{kk}_{i1}$ is the similar for the propagator with the spin-down.

$\circ \equiv L^{lat}_i$ is the crystal field Eqn (4).

$\sim\sim \equiv t_{i1i2}$ is the matrix of transfer Eqn (5).

The sets (13) and (14) after summation reduce to

$$= \delta_{i1i2} g_{i1\uparrow}(i\omega_n) + \delta_{i1i2} g_{i1\uparrow}(i\omega_n) L^{lat}_{i1} g_{i1\uparrow}(i\omega_n) + ... =$$

$$= \delta_{i1i2} \sum_k \frac{g^k_{i1\uparrow} X^{kk}_{i1}}{1 - L^{lat(k)}_{i1i1} g^k_{i1\uparrow}}, \qquad (17)$$

and

$$= \delta_{i1i2} g_{i1\downarrow}(i\omega_n) + \delta_{i1i2} g_{i1\downarrow}(i\omega_n) L^{lat}_{i1} g_{i1\downarrow}(i\omega_n) + ... =$$

$$= \delta_{i1i2} \sum_k \frac{g^k_{i1\downarrow} X^{kk}_{i1}}{1 - L^{lat(k)}_{i1i1} g^k_{i1\downarrow}} \qquad (18)$$

respectively.

Now we can write the Dyson equations for the electron propagator $g_{i\sigma}(i\omega_n) = \sum_k g^k_{i\sigma}(i\omega_n) X^{kk}_i$:

$=$ $+$ $\Sigma^{\uparrow}$, (19)

and for the electron propagator $g^k_{i\sigma}(i\omega_n) = \frac{1}{i\omega_n - \varepsilon_k - \Sigma^{\sigma}_{i(k)}(i\omega_n)}$:

$=$ $+$ $\Sigma^{\downarrow}$. (20)

One can notice that the self-energy part of the propagator Σ^{σ}_i occurs to be a single nodal following the DMFA[22]. The calculation of such local self-energy parts is performed in Appendix I.

4. Averaging of the Green's functions over configurations

In order to perform the averaging over the X operators the electron DOS operator $\hat{\rho}_X$ can be written as

$$\hat{\rho}_X = \prod_i \rho^i_X = \prod_i \left[(1-x) X^{AA}_i + x X^{MnMn}_i \right], \qquad (21)$$

where the A and Mn concentrations are determined through the averages of the X operators

$$< X^{kk}_i >_X = Sp_X (X^{kk}_i \rho^i_X) = c_k, \qquad (22)$$

with $c_A = 1 - x$, $c_{Mn} = x$.

For the averaged electron propagator $< g_{i\sigma} >_X$ one gets

$$< g_{i\sigma} >_X = Sp_X (g_{i\sigma} \hat{\rho}_X) \approx c_A g^A_{i\sigma} + c_{Mn} g^{Mn}_{i\sigma}. \qquad (23)$$

Equation (23) is the approximate one that corresponds to the alloy approximation and does not take into account the correlation effects.

Averaging the Green's function we use the cumulant decompositions [10–13]

$$S^{(\sigma)} = < e^{\varsigma_1 g_{i\sigma} + \varsigma_2 L^{lat}_i} > = \exp\Big(\sum_{\substack{n,m \\ n+m>0}} \frac{[\varsigma_1]^n [\varsigma_2]^m}{n!\,m!} M^{\sigma}{}_{nm} \Big), \qquad (24)$$

where $M^{\sigma}{}_{nm} = \frac{\partial^n}{\partial \varsigma_1{}^n} \frac{\partial^m}{\partial \varsigma_2{}^m} S^{(\sigma)}{}_{|\varsigma_1 = \varsigma_2 = 0}$.

The node corresponding to the $M^{\sigma}{}_{nm}$ cumulant gathers the $n + m$ separate parts in the electron propagator $g_{i\sigma}(i\omega_n)$, e.g.

$M^{\uparrow}{}_{10} =$ $= < g_{i\uparrow} >_X$;

$M^{\uparrow}{}_{20} =$ $-$

$$- < (M^{\uparrow}{}_{10} - g^A_{i\uparrow})(M^{\uparrow}{}_{10} - g^{Mn}_{i\uparrow}) >, \qquad (25)$$

$M^{\uparrow}_{01} = M^{\downarrow}_{01} = < L^{lat}_i > =$.

Resulting from the configuration averaging of the Green's functions $< G^{\sigma}_i >$ given by the graphical expressions (13) and (14) one gets the following diagrams

1 *2* *3* *4*

; ; ; ;.... (26)

In this study we consider solely the diagrams for which the configuration averaging embraces the electron propagators and the crystal field separately (diagrams 1 and 2, see (26)). Such averaging is equivalent to the statement of the coherent potential independence on the self-consistent field. The Green's functions become renormalized, but new poles do not arise. The configuration averaging of each line can be performed in different ways (the cluster approximation, the averaging of independent field, and so on). Therefore it is suitable to introduce the special notation of such renormalized Green's function like

$$< g_{i\sigma}(i\omega_n) > = = < > =$$

$$= \sum_k < \frac{X^{kk}_i}{\left[g^k_{i\sigma}(i\omega_n) \right]^{-1} - L^{lat}_i} >. \qquad (27)$$

In the cluster approximation one has:

$$D_{i\sigma}{}^k(i\omega_n) \equiv < \frac{1}{\left[g^k_{i\sigma}(i\omega_n) \right]^{-1} - L^{lat}_i} > =$$

$$= \sum_{r=0}^{l} \frac{w(r)}{\left[g^k_{i\sigma}(i\omega_n) \right]^{-1} - (l-r)\lambda^{kk}_{ij} - r\lambda^{kk'}_{ij}}, \qquad (28)$$

where $w(r) = \frac{l!}{r!(l-r)!} c^r_k c^{l-r}_{k'}; k \neq k; k, k' = A, Mn$. l is the number of the nearest neighbors; i, j denote the nearest nodes of the $A_{1-x}Mn_x$ sub-lattice.

The further averaging over the transfer matrices leads to the equation for the averaged Green's function,

$$< G^{\sigma}_{i1i2} >_{i\omega_n} = \Xi^{\sigma}_{i1i2}(i\omega_n) + \\ + \sum_{i3,i4} \Xi^{\sigma}_{i1i3}(i\omega_n) t_{i3i4} < G^{\sigma}_{i4i2} >_{i\omega_n}. \quad (29)$$

Here the Ξ^{σ}_{i1i2} term is the self-energy part of the averaged Green's function (irreducible by transfer) for whole crystal that has the following diagram representation:

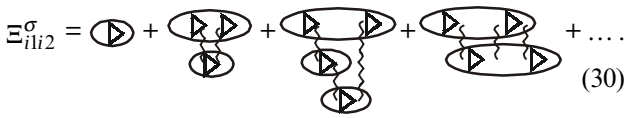

(30)

Let us retain the diagrams in the Ξ^{σ}_{i1i2} expression (30) of the single node nature solely (e.g. 1, 2, 3 and so on). Such procedure corresponds to the DMFT approximation or to the approximation of self-returning paths [14-16]. Then equation (30) can be rewritten in the form

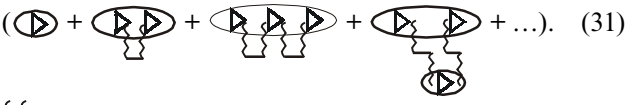

(31)

$\{\{\}\} \equiv J^{\sigma}$ is the sum of all diagrams beginning and terminating at the same node and having no common cumulants. The set (31) can be calculated analytically using equation (25). Thus,

$$\Xi^{\sigma}_i = \frac{c_A D^A + c_{Mn} D^{Mn} - D^A D^{Mn} J^{\sigma}}{1 - \left(c_A D^A + c_{Mn} D^{Mn}\right) J^{\sigma}}. \quad (32)$$

On the other hand, the sum J^{σ} can be determined if one finds the sum of all diagrams beginning and terminating at the same node and having the common cumulants:

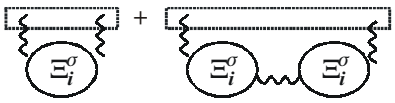

$$\frac{1}{N}\sum_{\vec{k}} t_{\vec{k}} \Xi^{\sigma}_i(i\omega_n) + \frac{1}{N}\sum_{\vec{k}} t^2_{\vec{k}} \left[\Xi^{\sigma}_i(i\omega_n)\right]^2 + \ldots = \quad (33)$$

$$= \frac{1}{N}\sum_{\vec{k}} \frac{\left[t_{\vec{k}}\right]^2}{\left[\Xi^{\sigma}_i(i\omega_n)\right]^{-1} - t_{\vec{k}}},$$

where $t_{\vec{k}} = \sum_{ij} e^{-\vec{k}(\vec{R}_i - \vec{R}_j)} t_{ij}$ is the Fourier transform of the transfer matrix.

It is clear that the sum (33) is equal to

$$\frac{1}{N}\sum_{\vec{k}} \frac{\left[t_{\vec{k}}\right]^2}{\left[\Xi^{\sigma}_i(i\omega_n)\right]^{-1} - t_{\vec{k}}} = J^{\sigma}_i(i\omega_n)\left\{1 - \Xi^{\sigma}_i(i\omega_n) J^{\sigma}_i(i\omega_n)\right\}. \quad (34)$$

Let us rewrite the expressions (29), (33), and (34) in the traditional form of the equations for the coherent potential as follows:

$$< G^{\sigma}_i(i\omega_n) >= \frac{1}{N}\sum_{\vec{k}} < G^{\sigma}_{\vec{k}}(i\omega_n) >= \\ = \frac{1}{N}\sum_{\vec{k}} \frac{1}{\left[\Xi^{\sigma}_i(i\omega_n)\right]^{-1} - t_{\vec{k}}}, \quad (35)$$

Then the coherent potential $J^{\sigma}_i(i\omega_n)$ takes the form

$$J^{\sigma}_i(i\omega_n) = \left[\Xi^{\sigma}_i(i\omega_n)\right]^{-1} - \left[< G^{\sigma}_i(i\omega_n) >\right]^{-1}. \quad (36)$$

Thus, solving the single node problems (19) and (20) (see Appendix I) one gets the solution of the self-consistent problem for the $A_{1-x}Mn_x$ sub-lattice.

5. Numerical results

In order to complete the CPA equations ((35) and (36)) the explicit expressions for the local single node self-energy parts $\Sigma^{\sigma}_{i(k)}(i\omega)$ in the Dyson equations (19) and (20) must be derived. These parts define the peculiarities of the exchange interaction between an electron with the spin σ and the localized magnetic moment of the Mn ion. They can be found by projecting the Hamiltonian (1) on the Andersson-like Hamiltonian, the type of [17],

$$\hat{H}^{new} = \hat{H}_0 + V\sum_{i\sigma}(\xi_{1\sigma} a^+_{1i\sigma} + a_{1i\sigma}\xi^+_{1\sigma}) + \hat{H}_{\xi}, \quad (37)$$

where $\xi_{1\sigma}, \xi^+_{1\sigma}$ are the operators of annihilation and creation of an electron with the spin σ in the non-magnetic ion outside the i-th cluster, $\hat{H}_{\xi}$ is the Hamiltonian of vacuum.

The Hamiltonian $\hat{H}_0$ corresponds to the cluster consisting of the energies of magnetic (1) and non-magnetic (2) ions as shown in Fig. 1. We distinguish between the electron transfer over the properly non-magnetic atoms and that occurring within the cluster between the non-magnetic and magnetic atoms. This scenario seems to be reasonable in the case of strongly diluted magnetic semiconductors (SDMS). Thus the $\hat{H}_0$ part of the Hamiltonian (37) takes the explicit form:

$$\hat{H}_0 = \sum_{i\sigma}\varepsilon_A a^+_{1i\sigma} a_{1i\sigma} + \sum_{i\sigma}\varepsilon_{Mn} a^+_{2i\sigma} a_{2i\sigma} + \\ + \alpha\sum_{\sigma,\sigma'}(\vec{S}_i\vec{\sigma})_{\sigma\sigma'} a^+_{2i\sigma} a_{2i\sigma'} + \\ + ztS/(2S+1)\sum_{i\sigma}(a^+_{2i\sigma} a_{1i\sigma} + c.c). \quad (38)$$

The self-energy parts for the Dyson equations (19) and (20) are defined by relations:

$$<< a_{1\sigma} \mid a^+_{1\sigma} >>_{\omega} = \frac{1}{\omega - \varepsilon_A - \Sigma^{\sigma}_{i(A)}(\omega)}, \quad (39)$$

$$<< a_{2\sigma} \mid a^+_{2\sigma} >>_{\omega} = \frac{1}{\omega - \varepsilon_{Mn} - \Sigma^{\sigma}_{i(Mn)}(\omega)}, \quad (40)$$

and the coherent potential $J_{\sigma}(\omega)$ is determined through the Baym-Kadanoff field [18] as follows [17]:

$$J_{\sigma}(\omega) = 2\pi V^2 << \xi_{1\sigma} \mid \xi^+_{1\sigma} >>_{\omega}. \quad (40)$$

The $<< a_{1\sigma} \mid a^+_{1\sigma} >>_{\omega}$ and $<< a_{2\sigma} \mid a^+_{2\sigma} >>_{\omega}$ Green's functions finding is given in Appendix I. Starting the SDMS investigation one can use the spin-polaron approximation of the single node Hamiltonian developed in Ref [19]. Ne-

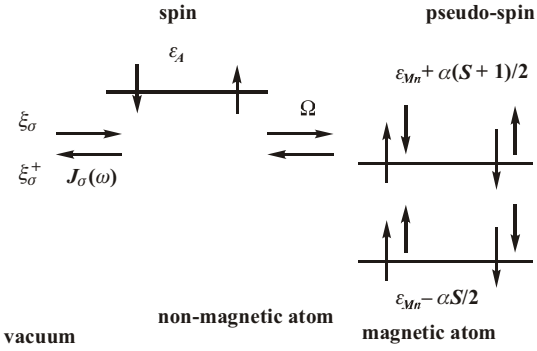

Fig. 1. The "cluster" consisting of two atoms, magnetic and non-magnetic. At the magnetic atom there are the spins up and down corresponding to the energies $\varepsilon_d - \frac{\alpha S}{2}$ and $\varepsilon_d + \frac{\alpha(S+1)}{2}$ respectively. The level ε_A is degenerate by spin at the non-magnetic atom.

glecting transverse components of the classical spins the single node Hamiltonian can be written in the form [19]:

$$H_0 = \sum_{i\sigma} \varepsilon_A a^+_{1i\sigma} a_{1i\sigma} + \sum_{i\sigma} \varepsilon^\sigma a^+_{2i\sigma} a_{2i\sigma} + \\ + ztS/(2S+1) \sum_{i\sigma} (1 + S_i^z / S)(a^+_{2i\sigma} a_{1i\sigma} + c.c). \quad (41)$$

For the sake of simplicity, we introduce the common notation σ both for the pseudo-spin, if the electron is at the magnetic atom (2), and for the spin, if it is at the non-magnetic atom (1). $\varepsilon^{\sigma=1/2} = \varepsilon_{Mn} - \alpha S/2$ is the energy of the spin-polaron with the pseudo-spin σ = 1/2 and $\varepsilon^{\sigma=-1/2} = \varepsilon_{Mn} + \alpha(S+1)/2$ is the energy for the pseudo-spin $-\sigma$ = 1/2. Introducing the Hamiltonian (10) we modify somewhat the effect of magnetic field on the $A_{1-x}Mn_xB$ semiconductor similarly to the effect of magnetic field in the transverse Ising model.

In what follows, we calculate the electron spectrum basing on the self-consistent solution of the set of equations (32), (35), (36), and (A.9), (A.19) for the DFTA technique [22], that reduces equation (35) to the form:

$$\frac{1}{N}\sum_{\vec{k}} \frac{1}{\left[\Xi_i^\sigma(i\omega_n)\right]^{-1} - t_{\vec{k}}} = \int_{\varepsilon_{\min}}^{\varepsilon_{\max}} \frac{\rho(\varepsilon)}{\left[\Xi_i^\sigma(i\omega_n)\right]^{-1} - \varepsilon}. \quad (42)$$

The DOS function for free electron states is approximated with $\rho(\varepsilon) = \frac{2}{\pi W^2}\sqrt{W^2 - \varepsilon^2}$ in case of the semi-elliptic Bethe lattice, and with $\rho(\varepsilon) = \frac{1}{W\sqrt{\pi}} e^{-\left(\frac{\varepsilon}{W}\right)^2}$ in case of the cubic lattice.

The iteration procedure is exploited in order to get the solution. At the first stage the zero approximation for the coherent potential $J_\sigma(\omega)$ is taken and the expression $\Xi_\sigma(\omega)$ is calculated from the equation (32). The single node local propagators $D_\sigma^A(\omega)$ and $D_\sigma^{Mn}(\omega)$ are defined using the expressions (A.9) and (A.19) if the crystal field (28) is neglected. Then using the relation between the averaged Green's function and the Green's function of whole crystal (35), and the model DOS functions (5.7) the averaged Green's function $\langle G_\sigma(\omega)\rangle$ is calculated. Then the coherent potential $J_\sigma(\omega)$ is re-defined using the relation (36). This re-defined potential serves again as the zero approximation potential, and the next loop of the calculation is fulfilled. In this scheme it is of great importance to find an appropriate expression of the coherent potential for the zero approximation. To this end the particular algebraic equation has been solved. This equation was derived in the semi-elliptic case and in case of the alloy approximation for the $\Xi_\sigma(\omega)$ corresponding to the simplified expression (28):

$$\Xi_i^\sigma(\omega) = (1-x)D_\sigma^A(\omega) + xD_\sigma^{Mn}(\omega). \quad (43)$$

Similar approximation was used in Ref. [3].

The dependences of the band centers on the ε_{Mn} energy for non-magnetic and magnetic atoms calculated from the equations (A.8) are depicted in Fig. 2. It can be seen that in case of a deep position of the Mn^{2+} energy levels the positions of the conduction band center for different spins are very close, whereas the centers of bands which are formed with the Mn^{2+} participation are split by the spin-polaron energy αS. If the manganese levels move upper the complicated scheme of splitting is observed [9]. While the analysis of the cluster with the Hamiltonian (41) is performed in the mean field approximation for the magnetic sub-system, the effect of additional magnetization $< S^z > \neq 0$ reduces to the additional shift of the band centers in Fig. 2 due to the change of the electron hopping rate between magnetic and non-magnetic atoms interior the cluster (A.2).

The edges of the formed bands demonstrate more complicated behavior. Indeed, the semi-elliptic band in the alloy approximation (43) that is the partial case of expression (28) has been considered in Ref. [3]. It was shown the existence of the induced ferromagnetism due to a complicated structure of the band edge that is sensitive to the change of the magnetization $\langle S^z \rangle / S$ of the magnetic sub-system. This structure manifests itself not only in the edge transformation, but in the formation of new bands also. The value of the ratio $\alpha S/W$, $\alpha S/W < 1$ for the case of DMS, is of importance for the development of the structure. It has been shown that for magnetic atoms the narrow bands with different spins arise in the spin-polaron approximation whereas for the conduction bands with different spins the DOS functions nearly coincide. It follows that the conduction band is significantly narrower due to the correlation effects (if $x \to 0$, $W \to W/\sqrt{6}$) [14–16, 20, 21]. If x increases, the conduction band width (determined by non-magnetic atoms) has to be smaller, whereas the spin-polaron states (related to magnetic atoms) broaden out. Besides the additional sub-bands arise near the conduction band as well as the resonant states appear interior the conduction band due to more complicated scattering processes amplified by correlation.

In order to fall outside the limits of the alloy approximation (43), the more complicated cumulants basing on

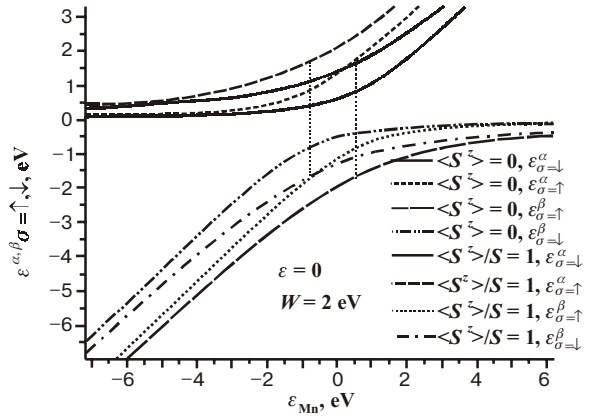

Fig. 2. Dependences of the band centers $\varepsilon_\sigma^{\alpha,\beta}$ on the energies ε_{Mn} in the case of the fixed value $\varepsilon_A = 0$. These dependences are found from (A.8) for two limiting cases: paramagnetic $\langle S^z \rangle / S = 0$ and saturated ferromagnetic $\langle S^z \rangle / S = 1$.

the equation (32) have to be taken into account. Fig. 3 shows the electron DOS dependences on energy for non-magnetic atoms if three different approximations are considered. In case of the elliptical DOS (Fig. 4), the correlation squeezing of the band decreases and the additional sub-band forms the edge of the conduction band beyond the alloy approximation. In the case of the gauss DOS (Fig. 5), the band undergoes even smaller correlation squeezing. Comparing the results for elliptical and gauss densities we find that the edge of the conduction band behaves itself very similarly in both cases. However, the elliptic band becomes narrower in comparison with the gauss band, thus providing better facility to see the additional sub-bands. Besides, the more complicated structures arise near the edges of the conduction band (Fig.5). Such structures are absent for spin-up states.

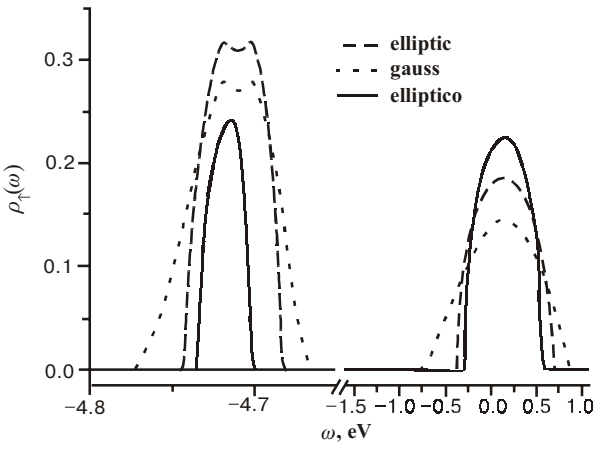

Fig. 3. Dependences of the electron DOS on the energy for the states with the spin up calculated in the alloy approximation (43) and the elliptic band, taking into account the higher cumulants (32) and the elliptic band, and assuming the higher cumulants contribution and the gauss density for the set of parameters: $W = 2$ eV, $x = 0.1$, $\varepsilon_A = 0$, $\varepsilon_{Mn} = -2W$, $\alpha = 0.45$, $\langle S^z \rangle / S = 0$ (non-magnetic atoms).

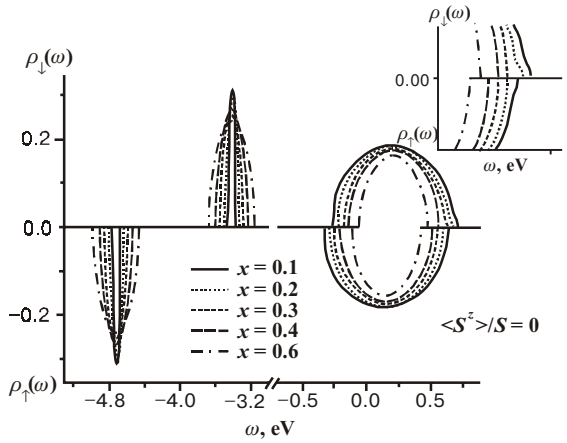

Fig. 4. Electron DOS dependences on the energy in the $A_{1-x}Mn_xB$ semiconductor calculated assuming the higher cumulants contribution and the elliptic band at $W = 2$ eV, $x = 0.1$; $x = 0.2$; $x = 0.3$; $x = 0.4$; $x = 0.6$, $\varepsilon_A = 0$, $\varepsilon_{Mn} = -2W$, $\alpha = 0.45$ and $\langle S^z \rangle / S = 0$.

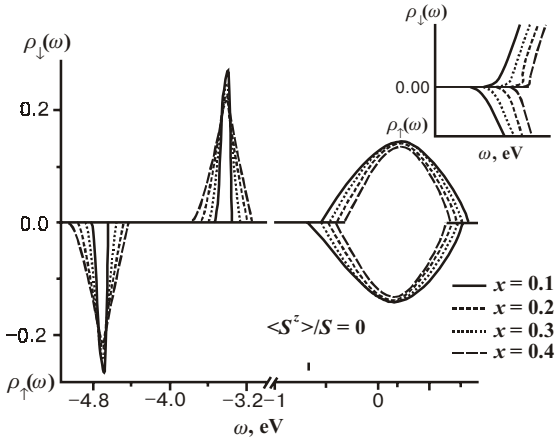

Fig. 5. Electron DOS dependences on the energy in the $A_{1-x}Mn_xB$ semiconductor calculated subject to the higher cumulants (32) and the gauss band at $W = 2$ eV, $x = 0.1$; $x = 0.2$; $x = 0.3$; $x = 0.4$, $\varepsilon_A = 0$, $\varepsilon_{Mn} = -2W$, $\alpha = 0.45$ and $\langle S^z \rangle / S = 0$.

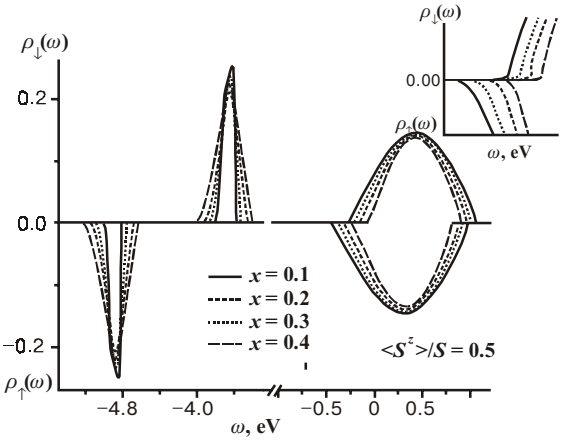

Fig. 6. Electron DOS dependences on energy in the $A_{1-x}Mn_xB$ semiconductor calculated assuming the higher cumulants contribution (32) and the gauss band at $W = 2$ eV, $x = 0.1$; $x = 0.2$; $x = 0.3$; $x = 0.4$, $\varepsilon_A = 0$, $\varepsilon_{Mn} = -2W$, $\alpha = 0.45$ and $\langle S^z \rangle / S = 0.5$.

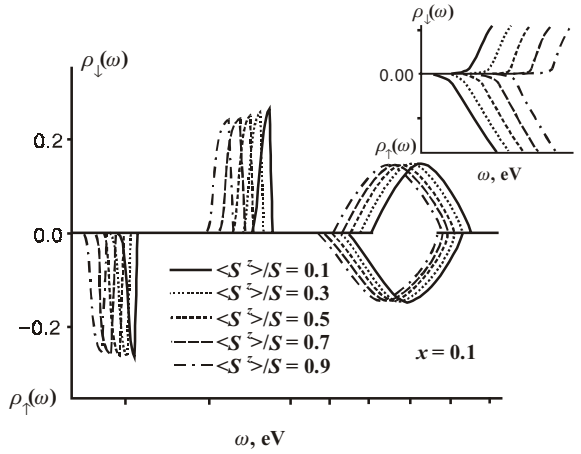

Fig. 7. Electron DOS dependences on the energy in the $A_{1-x}Mn_xB$ semiconductor calculated subject to the higher cumulants (32) and the gauss band at W = 2 eV, $x = 0.1$, $\varepsilon_A = 0$, $\varepsilon_{Mn} = -2W$, $\alpha = 0.45$ and $\langle S^z\rangle/S = 0.1$; $\langle S^z\rangle/S = 0.3$; $\langle S^z\rangle/S = 0.5$; $\langle S^z\rangle/S = 0.7$; $\langle S^z\rangle/S = 0.9$.

All dependences given above have been calculated for the case $< S^z > / S = 0$. It is clear that the single node problem solved in Appendix I is oversimplified to be used for the investigation of the spin correlations. Under such approach the introduction of $< S^z > / S \neq 0$ could result in a shift of the band centers (A.8) (see, Fig. 2), that in turn can magnify the band edges for smaller x with respect to the case $< S^z > / S = 0$ (Fig. 6). Thus, the principal effect of $< S^z > / S \neq 0$ is the DOS change near the band edges, whereas the band profile does not change (Fig. 7).

6. Conclusions

There exist a number of points differing the class of SDMS the type of $A_{1-x}Mn_xB$ from other classes of magnetic materials (spin glasses, diluted Heisenberg magnets, weakly ferromagnetic semiconductors, etc.): i) the peculiarities of SDMS are determined by the peculiarities of the electron band structure. The magnetism disposed experimentally in this class of semiconductors belongs to the interior type of magnetism making it contiguous to the Hubbard class of materials; ii) since at high x concentrations of the transition metal the formation of clusters is unavoidable, the theory has to be developed for the range of concentrations $x < x_c$. The percolation concentration x_c is the constant depending on the space dimensionality d and on the type of the crystal lattice, i.e. for $d = 3$, $0.1 < x < 0.3$. For the $A_{1-x}Mn_xB$ semiconductors at the random distribution of the magnetic component over the crystal lattice is of importance that makes the investigation of these systems basing upon the diluted Heisenberg model inadequate. In this model the formation of the Curie temperature T_c occurs due to the long-range order whereas for the SDMS the T_c formation is contributed by the short-range ordering magnified by magnetic fluctuations; iii) the magnetic momentum of the Mn^{2+} ion in AB lattice behaves itself similarly to the case of free Mn^{2+} ions. Thus the magnetic sub-system of the strongly diluted $A_{1-x}Mn_xB$ semiconductors can be described using the Hamiltonian like the Vonsovskii Hamiltonian.

The self-consistent formalism developed in this paper takes into account all above-mentioned points. It can be considered as a first step to the problem of magnetism in the SDMS. In our consideration of the model Hamiltonian we do not use the great canonical distribution. It means that the electronic sub-system is considered at zero temperatures, whereas the temperature effect on the magnetic sub-system is taken in the mean field approximation (A.2). The conduction band plays here the formal role, while rather the single-band model of semiconductor is used. The development of the multiple band theory based on the coherent potential is in progress. It is clear that the cluster approximation has to be extended to seek the Green's functions of the spin operators [1, 2]. In the developed model the correlation band squeezing is observed in contrast to the model [3] where the band edges follow the Hubbard model in the alloy approximation. It is of importance to take into account the Coulomb repulsion of the electrons with opposite spins at the magnetic atom [6–8]. This repulsion can substantially change the behavior of SDMS at least at certain relations between three parameters W, U, αS available in such models.

Appendix 1. Single-node Hamiltonian for the $A_{1-x}Mn_xB$ compounds

The Hamiltonian in the node representation can be written as

$$\hat{H}^{new} = \hat{H}_0 + V\sum_{i\sigma}(\xi_{1\sigma}a^+_{1i\sigma} + a_{1i\sigma}\xi^+_{1\sigma}) + H_\xi, \qquad (A.1)$$

where

$$\hat{H}_0 = \sum_{i\sigma}\varepsilon_A a^+_{1i\sigma}a_{1i\sigma} + \sum_{i\sigma}\varepsilon^\sigma a^+_{2i\sigma}a_{2i\sigma} +$$
$$+ ztS/(2S+1)\sum_{i\sigma}(1 + S^z_i/S)(a^+_{2i\sigma}a_{1i\sigma} + c.c)$$

and

$$\varepsilon^{\sigma=1/2} = \varepsilon_{Mn} - \alpha S/2\,,\ \varepsilon^{\sigma=-1/2} = \varepsilon_{Mn} + \alpha(S+1)/2\,.$$

While the localized spin moments follow the paramagnetic gas behavior we use the mean field approximation assuming that the magnetic field influences the cluster changing only the rate of hopping between the magnetic and non-magnetic ions. In this case the expression reduces to the form

$$\hat{H}_0 = \sum_{i\sigma}\varepsilon_A a^+_{1i\sigma}a_{1i\sigma} + \sum_{i\sigma}\varepsilon^\sigma a^+_{2i\sigma}a_{2i\sigma} +$$
$$+ \Omega\sum_{i\sigma}(a^+_{2i\sigma}a_{1i\sigma} + c.c), \qquad (A.2)$$

with the $\Omega = ztS/(2S+1)(1+ < S^z > / S)$.

In fact the Hamiltonian $\hat{H}^{new}$ is composed in such way that for the averaged Green function determined by the CPA technique the following equality takes place

$$< \exp(-\beta\hat{H}^{new} >^{(H_\xi)} = \exp(-\beta\hat{H}_{eff})\,. \qquad (A.3)$$

Within the CPA technique the transition to the statistic operator is performed as follows:

$$e^{-\beta\hat{H}} \to e^{-\beta\hat{H}_{eff}} =$$
$$= e^{-\beta\hat{H}_0} \exp\left\{-\int_0^\beta d\tau_1 \int_0^\beta d\tau_2 \sum_\sigma J_\sigma(\tau_1-\tau_2) a_{1\sigma}^+(\tau_1) a_{1\sigma}(\tau_2)\right\}. \quad (A.4)$$

In terms of Green functions this procedure generates the self-consistent set of equations

$$< G^\sigma(\omega) >= \frac{1}{N}\sum_{\vec{k}} < G_{\vec{k}}^\sigma(\omega) >= \frac{1}{N}\sum_{\vec{k}} \frac{1}{\left[\Xi^\sigma(\omega)\right]^{-1} - t_{\vec{k}}},$$
$$J_\sigma(\omega) = \left[\Xi^\sigma(\omega)\right]^{-1} - \left[< G^\sigma(\omega) >\right]^{-1}, \quad (A.5)$$

where the $J_\sigma(\omega) = 2\pi V^2 << \xi_{1\sigma} \mid \xi_{1\sigma}^+ >>_\omega$ is the dynamic Baym–Kadanoff field. Under the assumption of the $\Xi^\sigma(\omega)$ function, independent on the $\vec{k}$ vector, the set (A.5) gives also the DMFT set [15, 16].

Thus the (A.5) set determines a dependence of the averaged Green function of the coherent potential,

$$< G^\sigma(\omega) >= f(J_\sigma(\omega)). \quad (A.6)$$

The transformation

$$a_{1i\sigma} = \cos\left(\frac{\theta_\sigma}{2}\right)\alpha_{i\sigma} + \sin\left(\frac{\theta_\sigma}{2}\right)\beta_{i\sigma},$$
$$a_{2i\sigma} = -\sin\left(\frac{\theta_\sigma}{2}\right)\alpha_{i\sigma} + \cos\left(\frac{\theta_\sigma}{2}\right)\beta_{i\sigma} \quad (A.7)$$

reduces the $\hat{H}_0$ to the diagonal form

$$\hat{H}_0 = \sum_{i\sigma} \varepsilon_\sigma^\alpha \alpha_{i\sigma}^+ \alpha_{i\sigma} + \sum_{i\sigma} \varepsilon_\sigma^\beta \beta_{i\sigma}^+ \beta_{i\sigma}. \quad (A.8)$$

Here $\varepsilon_\sigma^\alpha = \varepsilon_A - (\varepsilon_A - \varepsilon^\sigma)\sin^2\left(\frac{\theta_\sigma}{2}\right) - \Omega\sin(\theta_\sigma)$,

$\varepsilon_\sigma^\beta = \varepsilon^\sigma + (\varepsilon_A - \varepsilon^\sigma)\sin^2\left(\frac{\theta_\sigma}{2}\right) + \Omega\sin(\theta_\sigma)$,

and $tg(\theta_\sigma) = -\frac{2\Omega}{\varepsilon_A - \varepsilon^\sigma}$.

In order to find the Green functions $<< a_{1\sigma} \mid a_{1\sigma}^+ >>_\omega$ and $<< a_{2\sigma} \mid a_{2\sigma}^+ >>_\omega$, one needs to find the Green functions $<< \alpha_\sigma \mid \alpha_\sigma^+ >>_\omega$ and $<< \beta_\sigma \mid \beta_\sigma^+ >>_\omega$. Indeed,

$$<< a_{1\sigma} \mid a_{1\sigma}^+ >>_\omega = \cos^2\left(\frac{\theta_\sigma}{2}\right) << \alpha_\sigma \mid \alpha_\sigma^+ >>_\omega +$$
$$+ \frac{\sin(\theta_\sigma)}{2}(<< \alpha_\sigma \mid \beta_\sigma^+ >>_\omega + << \beta_\sigma \mid \alpha_\sigma^+ >>_\omega) +$$
$$+ \sin^2\left(\frac{\theta_\sigma}{2}\right) << \beta_\sigma \mid \beta_\sigma^+ >>_\omega,$$
$$<< a_{2\sigma} \mid a_{2\sigma}^+ >>_\omega = \sin^2\left(\frac{\theta_\sigma}{2}\right) << \alpha_\sigma \mid \alpha_\sigma^+ >>_\omega -$$
$$- \frac{\sin(\theta_\sigma)}{2}(<< \alpha_\sigma \mid \beta_\sigma^+ >>_\omega + << \beta_\sigma \mid \alpha_\sigma^+ >>_\omega) +$$
$$+ \cos^2\left(\frac{\theta_\sigma}{2}\right) << \beta_\sigma \mid \beta_\sigma^+ >>_\omega. \quad (A.9)$$

Write the equations of motion for the operators α and β:

$$\left[\alpha_\sigma, \hat{H}^{new}\right] = \varepsilon_\sigma^\alpha \alpha_\sigma + V\cos\left(\frac{\theta_\sigma}{2}\right)\xi_\sigma,$$
$$\left[\beta_\sigma, \hat{H}^{new}\right] = \varepsilon_\sigma^\beta \beta_\sigma + V\sin\left(\frac{\theta_\sigma}{2}\right)\xi_\sigma,$$
$$\left[\alpha_\sigma^+, \hat{H}^{new}\right] = -\varepsilon_\sigma^\alpha \alpha_\sigma^+ - V\cos\left(\frac{\theta_\sigma}{2}\right)\xi_\sigma^+, \quad (A.10)$$
$$\left[\beta_\sigma^+, \hat{H}^{new}\right] = -\varepsilon_\sigma^\beta \beta_\sigma^+ - V\sin\left(\frac{\theta_\sigma}{2}\right)\xi_\sigma^+$$

The generalized Wick theorem can be used to find the Green functions $<< \alpha_\sigma \mid \alpha_\sigma^+ >>_\omega$ and $<< \beta_\sigma \mid \beta_\sigma^+ >>_\omega$. This theorem in terms of the irreducible Green functions [17, 22] is formulated as follows

$$\left[\alpha_\sigma, \hat{H}^{new}\right] = \varepsilon_\sigma^\alpha \alpha_\sigma + \cos\left(\frac{\theta_\sigma}{2}\right)Z_\sigma^\alpha,$$
$$\left[\beta_\sigma, \hat{H}^{new}\right] = \varepsilon_\sigma^\beta \beta_\sigma + \sin\left(\frac{\theta_\sigma}{2}\right)Z_\sigma^\beta. \quad (A.11)$$

Here, $Z_\sigma^\alpha, Z_\sigma^\beta$, and $Z_\sigma^{\alpha+}, Z_\sigma^{\beta+}$ are the irreducible parts of the Green functions $<< \alpha_\sigma \mid \alpha_\sigma^+ >>_\omega$ and $<< \beta_\sigma \mid \beta_\sigma^+ >>_\omega$ respectively, and they can be written explicitly as

$$Z_\sigma^\alpha = V\xi_\sigma, \qquad Z_\sigma^\beta = V\xi_\sigma. \quad (A.11')$$

In order to rewrite the equations of motion in more compact form, the relations are used

$$\omega << \hat{A} \mid \hat{B} >>_\omega = \frac{1}{2\pi} < \left\{\hat{A}, \hat{B}\right\} > + << \left[\hat{A}, \hat{H}^{new}\right] \mid \hat{B} >>_\omega \text{ and}$$
$$\omega << \hat{A} \mid \hat{B} >>_\omega = \frac{1}{2\pi} < \left\{\hat{A}, \hat{B}\right\} > - << \hat{A} \mid \left[\hat{B}, \hat{H}^{new}\right] >>_\omega, \quad (A.12)$$

where $\hat{A} = \alpha_\sigma, \beta_\sigma$; $\hat{B} = \alpha_\sigma^+, \beta_\sigma^+$ and $\hbar = 1$.

Then

$$\hat{G} = \hat{G}_0 + \hat{G}_0 \hat{A}\hat{P}\hat{A}\hat{G}_0, \quad (A.13)$$

where $\hat{G} = \begin{pmatrix} << \alpha_\sigma \mid \alpha_\sigma^+ >>_\omega & << \alpha_\sigma \mid \beta_\sigma^+ >>_\omega \\ << \beta_\sigma \mid \alpha_\sigma^+ >>_\omega & << \beta_\sigma \mid \beta_\sigma^+ >>_\omega \end{pmatrix}$,

$$\hat{G}_0 = \begin{pmatrix} \frac{1/2\pi}{\omega - \varepsilon_\sigma^\alpha} & 0 \\ 0 & \frac{1/2\pi}{\omega - \varepsilon_\sigma^\beta} \end{pmatrix}, \quad \hat{A} = \begin{pmatrix} 2\pi\cos\frac{\theta_\sigma}{2} & 0 \\ 0 & 2\pi\sin\frac{\theta_\sigma}{2} \end{pmatrix},$$

and

$$\hat{P} = \begin{pmatrix} << Z_\sigma^\alpha \mid Z_\sigma^{\alpha+} >> & << Z_\sigma^\alpha \mid Z_\sigma^{\beta+} >> \\ << Z_\sigma^\beta \mid Z_\sigma^{\alpha+} >> & << Z_\sigma^\beta \mid Z_\sigma^{\beta+} >> \end{pmatrix}.$$

Let us transform the matrix equation (A.13) into the equation of the Dyson type transforming the mass operator according to

$$\hat{A}\hat{P}\hat{A} = \hat{M} + \hat{M}\hat{G}_0\hat{M} + \ldots, \quad (A.14)$$

where

$$\hat{M} = \hat{A}^{-1}\begin{pmatrix} {}^{irr}<< Z_\sigma^\alpha \mid Z_\sigma^{\alpha+} >>^{irr} & {}^{irr}<< Z_\sigma^\alpha \mid Z_\sigma^{\beta+} >>^{irr} \\ {}^{irr}<< Z_\sigma^\beta \mid Z_\sigma^{\alpha+} >>^{irr} & {}^{irr}<< Z_\sigma^\beta \mid Z_\sigma^{\beta+} >>^{irr} \end{pmatrix}\hat{A}^{-1}. \quad (A.15)$$

Thus one gets

$$\hat{G} = \hat{G}_0 + \hat{G}_0 \hat{M} \hat{G} \ . \qquad \text{(A.16)}$$

Irreducible parts of the Green functions can be calculated using the technique of two-time decoupling and the spectral theorem, e.g.

$$^{irr}<< Z_\sigma^\alpha \mid Z_\sigma^{\alpha+} >>^{irr} =$$

$$= \frac{1}{2\pi}\int_{-\infty}^{\infty} \frac{d\omega_1}{\omega - \omega_1}(e^{\beta\omega_1}+1)\int_{-\infty}^{\infty}\frac{dt}{2\pi}e^{-i\omega_1 t} <Z_\sigma^{\alpha+}(t) Z_\sigma^\alpha > . \qquad \text{(A.17)}$$

In the case of approximation (A.11′), the matrix (A.15), using (A.17) and (A.5), can be reduced to the form:

$$\hat{M} = \hat{A}\begin{pmatrix} \frac{1}{2\pi}J_\sigma(\omega) & \frac{1}{2\pi}J_\sigma(\omega) \\ \frac{1}{2\pi}J_\sigma(\omega) & \frac{1}{2\pi}J_\sigma(\omega) \end{pmatrix}\hat{A} . \qquad \text{(A.18)}$$

Solving matrix equations (A.16), the explicit expressions for the Green functions are found.

$$<<\alpha_\sigma \mid \alpha_\sigma^+ >>_\omega = \frac{1}{2\pi(\omega - \varepsilon_\sigma^\alpha) - J_\sigma(\omega)\cos^2\left(\frac{\theta_\sigma}{2}\right) - \frac{J^2{}_\sigma(\omega)\sin^2(\theta_\sigma)}{4(\omega - \varepsilon_\sigma^\beta - J_\sigma(\omega)\sin^2\left(\frac{\theta_\sigma}{2}\right)}},$$

$$<<\beta_\sigma \mid \beta_\sigma^+ >>_\omega = \frac{1}{2\pi(\omega - \varepsilon_\sigma^\beta) - J_\sigma(\omega)\sin^2\left(\frac{\theta_\sigma}{2}\right) - \frac{J^2{}_\sigma(\omega)\sin^2(\theta_\sigma)}{4(\omega - \varepsilon_\sigma^\alpha - J_\sigma(\omega)\cos^2\left(\frac{\theta_\sigma}{2}\right)}}, \qquad \text{(A.19)}$$

$$<<\beta_\sigma \mid \alpha_\sigma^+ >>_\omega = \frac{\sin(\theta_\sigma)J_\sigma(\omega)/2}{\left(2\pi(\omega - \varepsilon_\sigma^\alpha) - J_\sigma(\omega)\cos^2\left(\frac{\theta_\sigma}{2}\right)\right)\left(\omega - \varepsilon_\sigma^\beta - J_\sigma(\omega)\sin^2\left(\frac{\theta_\sigma}{2}\right)\right) - \frac{J^2{}_\sigma(\omega)\sin^2(\theta_\sigma)}{4}},$$

$$<<\alpha_\sigma \mid \beta_\sigma^+ >>_\omega = \frac{\sin(\theta_\sigma)J_\sigma(\omega)/2}{\left(2\pi(\omega - \varepsilon_\sigma^\beta) - J_\sigma(\omega)\sin^2\left(\frac{\theta_\sigma}{2}\right)\right)\left(\omega - \varepsilon_\sigma^\alpha - J_\sigma(\omega)\cos^2\left(\frac{\theta_\sigma}{2}\right)\right) - \frac{J^2{}_\sigma(\omega)\sin^2(\theta_\sigma)}{4}},$$

References

1. W. Nolting, S. Rex and S. Mathi Jaya, Magnetism and electronic structure of a local moment ferromagnet // *J. Phys. C*, **9**, pp. 1301-1330 (1997).
2. D. M. Edwards, A. C. M. Green and K. Kubo, Electronic structure and resistivity of the double exchange model // *J. Phys. C*, **11**, pp. 2791-2808 (1999).
3. M. Takahashi and K. Kubo, Coherent-potential approach to magnetic and chemical disorder in diluted magnetic semiconductors // *Phys. Rev. B*, **60**, pp.15858-15864 (1999).
4. M.P. Kennet, M. Berciu and R.N. Bhatt, Monte Carlo simulations of an impurity-band model for III-V diluted magnetic semiconductors // *Phys. Rev. B*, **66**, pp. 045207/1-16 (2002).
5. M. P. Kennett, M. Berciu, and R. N. Bhatt, Two-component approach for thermodynamic properties in diluted magnetic semiconductors // *Phys. Rev. B*, **65**, pp.115308/1-11 (2002).
6. V.A. Ivanov, P.M. Krstajic, F.M. Peeters, V.N. Fleurov, and K.A. Kikoin, On the nature of ferromagnetism in diluted magnetic semiconductors: GaAs:Mn, GaP:Mn // *Journal of Magnetism & Magnetic Materials*, **258-259**, pp. 237-240 (2003).
7. V.A. Ivanov, P. M. Krstajic, F. M. Peeters, V. N. Fleurov, and K. A. Kikoin, On the ferromagnetic exchange in Mn-doped III-V semiconductors // *Physica B*, **329-333**, pp.1282-1283 (2003).
8. P.M. Krstajic, F.M. Peeters, V.A. Ivanov, V. N. Fleurov and K. A. Kikoin, Double exchange mechanisms for Mn doped III-V ferromagnetic semiconductors // *Phys. Rev. B*, Submitted (2003).
9. K.A. Kikoin and V.N. Fleurov, Transition Metal Impurities in Semiconductors (World Scientific Publishing, Singapore) (1994).
10. R.N. Aiyer, R.J. Elliott, J.A. Krumhansl, and P.L. Leath, Pair Effects and Self-Consistent Corrections in Disordered Alloys //*Phys. Rev. B*, **181**, pp. 1006-1014 (1969);
11. F. Yonezawa, An exact form of first-order self-energy in random lattice problems // *Prog. Theor. Phys.*, **39**, pp. 1076-1078 (1968).
12. F. Yonezawa and T. Matsubara, Note on electronic state of random lattice II // *Prog. Theor. Phys.*, **35**, pp. 357-379 (1966);
13. F. Yonezawa, A systematic approach to the problems of random lattices I // *Prog. Theor. Phys.*, **40**, pp. 734-757 (1968).
14. W. Metzner; P. Schmit and D. Vollhardt, Hole dynamics a spin background: A sum-rule-conserving theory with exact limits//*Phys. Rev.* B, **45**, pp. 2237-2251 (1992).
15. Yu. A. Izyumov, The Hubbard model in the regime of strong electronic correlation // *Physics-Uspekhi*, **38**, pp. 385-410 (1995).
16. Yu. A. Izyumov, The *t–J* model for strongly correlated electrons and high-Tc superconductors // *Physics-Uspekhi*, **40**, pp. 445-477 (1997).
17. I.V. Stasyuk, Approximate analytical dynamical mean-field approach to strongly correlated electron systems// Condensed Matter Physics 3, pp. 437-455 (2000).
18. G. Baym and L.P. Kadanoff, Conservation laws and correlation functions // Phys.Rev. 124, pp. 287-299 (1961).
19. E.L. Nagayev, Electrons, indirect exchange and localized magnons in magnetoactive semiconductors // *ZhETP*, **56**, pp. 1013-1028 (1969).
20. M.I. Vladimir and V.A. Moskalenko, Diagram technique for the Hubbard model // *Theor. Math. Phys.*, **82**, pp. 428-437 (1990).
21. V.A. Moskalenko, Perturbation theory for nonperiodic Anderson model // *Theor. Math. Phys.*, **110**, pp. 308-322 (1997)
22. A.Georges, G.Kotliar, W.Krauth, and M.Rosenberg, Dynamical mean-field theory of strongly correlated fermion systems and the limit of infinite dimensions // *Rev. Mod. Phys.*, **68**, pp. 13-125 (1996).